A Scalable Method for the Synthesis of Metal Oxide Nanowires

J. Thangala, S. Vaddiraju, R. Bogale, R. Thurman, T. Powers, B. Deb, and M.K. Sunkara

Department of Chemical Engineering, University of Louisville, Louisville, KY 40292, USA

We report a novel, scaleable and versatile method for large scale synthesis of tungsten trioxide nanowires and their arrays on a variety of substrates including amorphous quartz, fluorinated tin oxide, etc. The synthesis concept uses the chemical vapor transport of metal oxide vapor phase species onto substrates using air or oxygen flow over hot-filament sources. The hot-filaments were designed to provide uniform heating and gas phase composition over large substrate areas. The results show that the nucleation densities could be varied from $10^6/cm^2$ to $10^{10}/cm^2$ with decreasing substrate temperature. A thermodynamic model for determining the nucleation density and nanowire diameter is presented. The analysis indicates that the nucleation for nanowires occurs through condensation of sub-oxide, WO_2 species. This is in contrast to WO_3 species condensation into WO_3 solid phase for nanoparticle formation. The dispersion behavior of as-synthesized nanowires in aqueous and organic solvents is also studied.

Introduction

Tungsten trioxide nanomaterials are of tremendous interest due to their potential use as electrochromic, gas sensing, and photocatalyst materials (1-3). The synthesis of doped and undoped tungsten oxide nanowires, using either tungsten foils or powders as sources, was reported previously in the literature (4-15). Previously, we reported a concept of utilizing chemical vapor transport of metal oxide vapor species using oxygen flow over hot-filaments onto substrates at different temperatures for both metal and metal oxide nanowires (5). In this vapor phase synthesis route, the chemical vapor transport of tungsten oxide onto substrates kept at temperatures higher than the decomposition temperature resulted in tungsten nanowires. Similar vapor transport of tungsten oxide onto substrates kept at temperatures below the decomposition resulted in tungsten oxide nanowire formation (5).

The synthesis of tungsten oxide nanowires is accomplished without the use of any catalysts or any medium. In essence, many of the synthesis studies including our studies indicated that the tungsten oxide nanowires resulted under a specific set of conditions within a chemical vapor deposition setup. So, we performed a systematic study to understand and optimize the tungsten oxide nanowire deposition process using a custom-built, hot-filament CVD reactor. We also present a thermodynamic model for assessing nanowire nucleation density as a function of various experimental variables such as substrate temperature, oxygen partial pressure and filament temperature, etc. In addition, we also conducted a series of experiments to study the nanowire dispersions in a variety of solvents and compared their behavior with that of commercially obtained nanoparticles.

Experimental

Figure 1 shows the schematic of the scaled-up version of the hot filament CVD reactor setup used for the synthesis studies. The setup consists of a 2-inch diameter quartz tube housed in a tube furnace heater. The ends of the quartz tube are connected to the necessary accessories for flow and pressure control. The filament used for the experiments is mounted on hollow ceramic rod as shown in Figure 1. A tungsten filament (Alfa Aesar) of 0.5mm diameter and 8 feet in length was used as the tungsten source in our experiments. The tungsten filament is heated up using an electrical feed-through to temperatures ranging from 1773 – 2273 K. The temperatures within our system were monitored using a dual wavelength pyrometer (Wilkinson, Model no. PRO 92-40-C-23) and another single wavelength pyrometer (Raytek, Model no. 2838780101). Quartz boats were employed to curtail the deposition directly onto the tube walls. Typically, the substrates (quartz and fluorinated tin oxide coated quartz slides) were placed on the boat as shown in the schematic. In the absence of the furnace heating, the radiation from hot-filaments directly heated the substrates to a maximum temperature of about 823 K. In another set of experiments, furnace heating was used to raise the substrate temperature from 1023 K till 1173 K. The feed gas composition was varied using pure oxygen or argon/air mixtures to change the partial pressure of oxygen from 0.1 torr to 0.000837 torr. The tungsten filament was always heated to a temperature of about 1950 K while maintaining the power (voltage and the current used for heating the filament) constant in all the experiments. Also, the duration of each synthesis experiment was kept at around 10-15 minutes unless specified.

The as-synthesized nanowires were collected in a dry powder form by scraping the material from the quartz substrates. The as-obtained nanowire powder was dispersed into four different solvents: water, ethanol, 1-methoxy 2-propanol and Dimethyl Formamide(DMF) using ultrasonication with a horn (UP200S Ultrasonic Processor) for two minutes followed by sonication in a low energy density bath for about 15 minutes. The dispersions were allowed to settle for few minutes and the initial sediments were taken out and weighed. The initial sediments always contained big particles, non-dispersed agglomerates and thicker nanowire bundles. The same procedure was implemented for all nanowire and nanoparticle (Aldrich) samples for dispersions into different solvents. The dispersions were allowed to settle over two days of time with continuous visual observations. The sediments were examined using SEM to observe the agglomeration patterns.

Results and Discussion

A set of experiments using substrates kept at temperatures around 823 K without using the furnace heater resulted in high nucleation density leading to a vertical array of WO_3 nanowires on both Quartz and FTO substrates. The synthesized tungsten oxide nanowires are all vertically aligned (Figure 2) with density as high as $7x10^{10}$ nw/cm^2. The x-ray diffraction (XRD) spectrum (Figure 3a) indicated that the as-synthesized bluish nanowire deposit was composed of an oxygen deficient $W_{18}O_{49}$ phase (JCPDS#05-0392, a=3.775A^o, c=13.98A^o and b=3.775A^o).
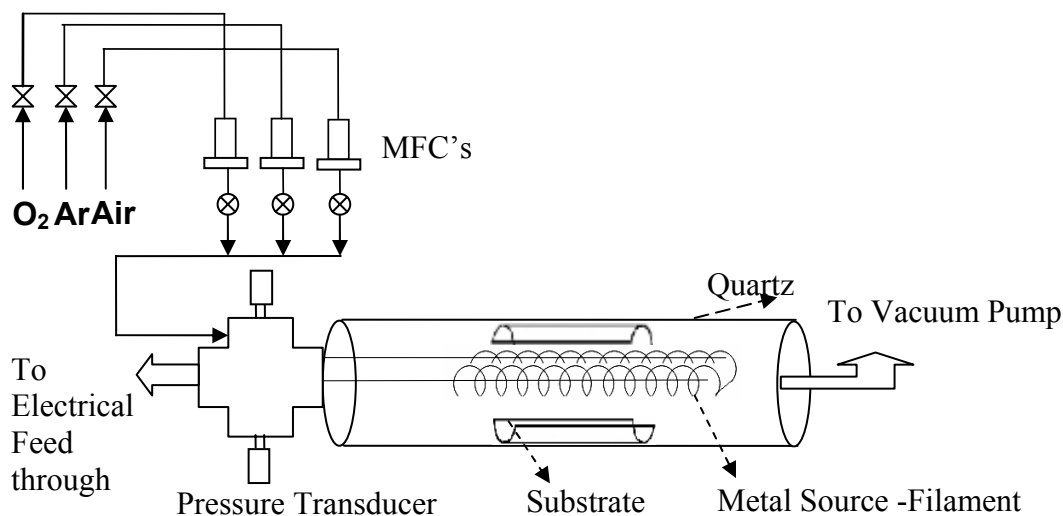
Figure 1. Schematic of the Scale up Hot Filament CVD reactor with tungsten filament inside the vacuum chamber
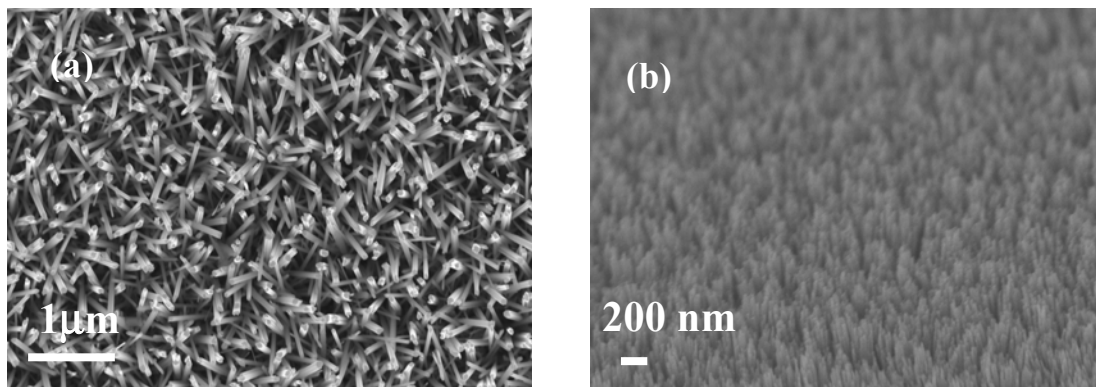

Figure 2. SEM images of as-synthesized tungsten oxide nanowires on top of the FTO substrate in presence of air (11sccm) and filament temperature (1950 K) for about 15 min. (a) Low magnification image of uniform deposition of tungsten oxide nanowires. (b) Tilted view of the sample showing uniform deposition of vertically aligned tungsten oxide arrays

Experiments conducted using 4 sccm of pure oxygen at a substrate temperature of 1073 K and a pressure of 0.5 torr, while maintaining the filaments at 1950 K, resulted in a yellowish green deposit on the substrate. The yellowish green deposit showed only the presence of nanoparticles (Figure 4a). The deposit obtained using air/argon mixture (0.4 sccm/100sccm) under similar conditions was bluish in color. The deposit (Figure 4b) contained nanowires of 40 nm in diameter and 5 microns in length. Oxidation of these nanowires in ambient atmosphere at a temperature of 773 K for about 30 minutes changed the color of the nanowires to yellow, and the corresponding XRD spectrum (Figure 3b) indicated that the phase of oxidized nanowires changed from $W_{18}O_{49}$ to WO_3 (JCPDS #20-1324; a = 7.384A^o, b = 7.512A^o, and c = 3.846A^o). At the same time, no structural damage or change is observed with the nanowires. These characteristics for

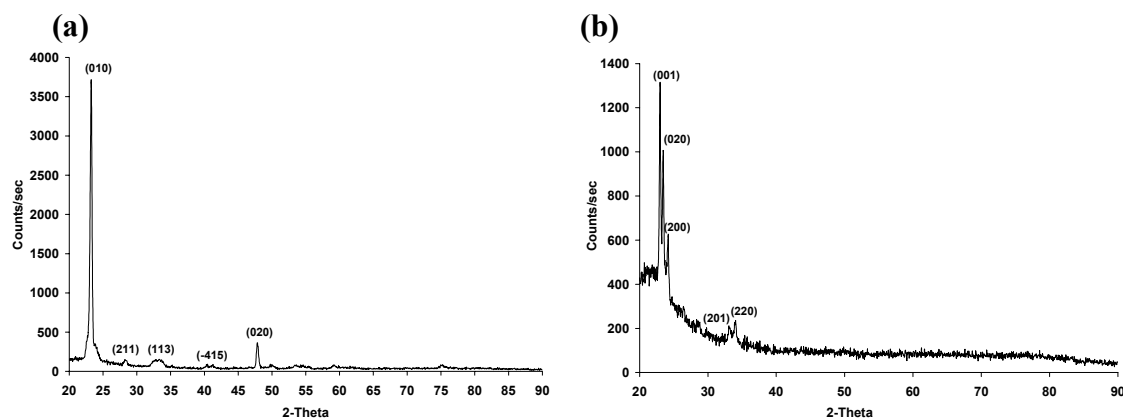tungsten oxide nanowires were found to be typical in all types of synthesis experiments performed.

Figure 3. XRD spectra of as-synthesized tungsten oxide nanowires. (a) Showing the spectra of as-synthesized tungsten oxide nanowires. (b) Showing the spectra of the oxidized tungsten oxide wires
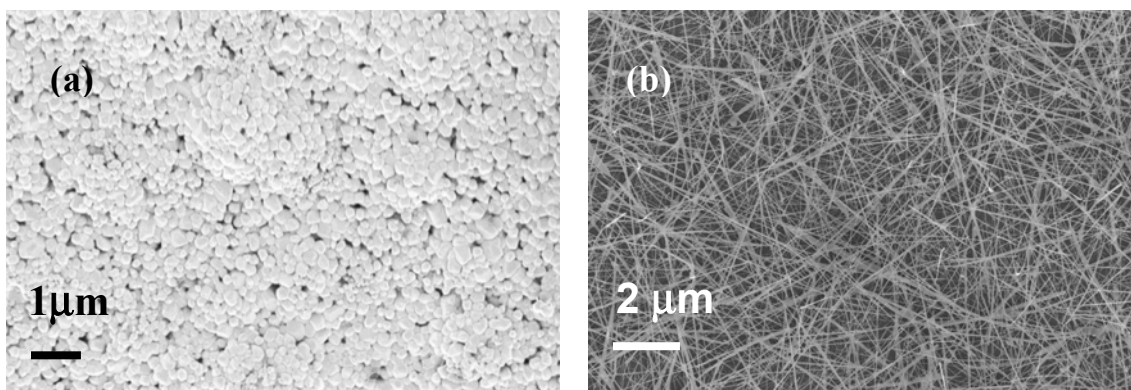

Figure 4. SEM images of tungsten oxide nanowires and nanoparticles (a) yellow deposit of nanoparticles obtained in presence of pure oxygen (2sccm), filament temperature of about 1950 K and substrate temperature of 1073 K. (b) blue deposit of nanowires of about 40nm and about 10 µm long in presence of Ar/air (100sccm/0.4sccm) and a filament temperature of about 1950 K and substrate temperature of 1073 K

A set of systematic experiments were performed to determine the effect of substrate temperature and oxygen partial pressure on the resulting nanowire density. During these experiments, the filament temperature was kept constant at about 1950 K. The results shown in Figure 4 and Figure 2 indicate that the nanowire density can be varied over several orders of magnitude by changing the substrate temperature. In all the experiments, the diameter of the nanowires varied between 30 to 60 nm. Higher partial pressures of oxygen, using the same substrate and filament temperatures (823 K and 1950 K respectively), led to the formation of high density of nanowires, bundled in the form of ball like structures. As shown in Figure 5, these structures consisted of nanowires, 20 nm in diameter and about 0.5 microns in length.
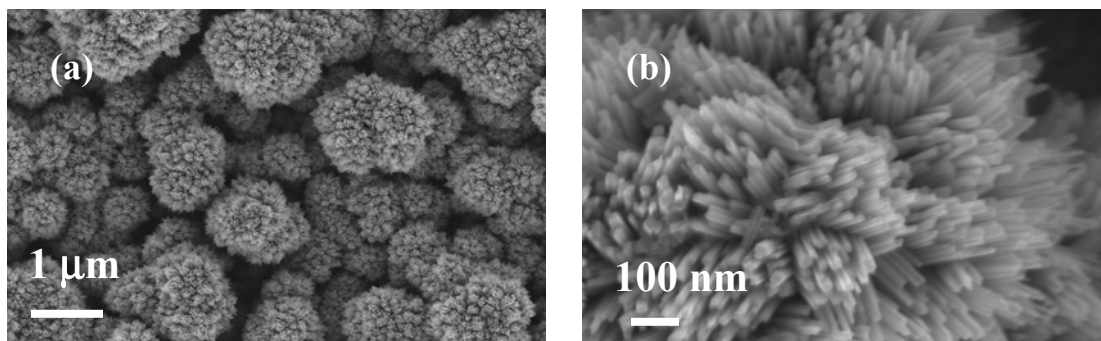
Figure 5. SEM images of high balls of low aspect ratio tungsten oxide nanowires synthesized at high pressure conditions (25 Torr). (a) Low magnification image showing several balls having several hundreds of nanowires in each ball kind of structure. (b) High magnification image showing nanowires in a single ball kind of structure with diameters in the range of 20 to 40nm

The nucleation of tungsten oxide from vapor phase could be understood by considering the vapor phase super-saturation. So, we determined the gas-solid equilibrium compositions at both filament and substrate temperatures for given oxygen partial pressures. Equilibrium calculations were performed using CHEMKIN 3.7.1 software. We considered W, WO, O, O_2, WO_2, WO_3 gas phase species and WO_2, W and WO_3 solid phases for gas-solid equilibrium computations. First, we assumed that the equilibrium exists at the filament temperatures. So, we computed the equilibrium compositions at filament temperature for a given set of feed gas composition and the reactor pressure conditions. Next, we assumed that there is no gas phase recombination or other gas phase reactions and no change in the composition in the gas phase. Finally, we also estimated the gas phase equilibrium composition at substrate. Based on the two compositions determined, we define the gas phase supersaturation for each of the vapor phase species present. Of the species considered, WO_3 species dominate the gas phase composition followed by WO_2 species. As indicated earlier (5), the critical diameter of the resulting tungsten oxide solid phase could be estimated using the following supersaturation,

$$d_c = 4\sigma\Omega / \left[RT \ln\left(\frac{p}{p^*} \right) \right]$$
[1]

Where σ is the interfacial energy, Ω is the molar volume, T is the substrate temperature, p is the partial pressure of the vapor phase oxide species, and p^* is the equilibrium vapor pressure of the vapor phase oxide species. The nucleation density of nanowires is inversely proportional to the critical diameter as seen below:

$$Nucleation\ Density\ \alpha\ \left[RT \ln\left(\frac{p}{p*} \right) \right]$$
[2]

The results indicate that the WO_3 species as the dominant species present but the supersaturation (p/p^*) values for WO_2 is much greater then that of WO_3. This would indicate that the WO_2 species condense readily giving rise to the sub-oxide phase clusters. Further growth of these clusters might proceed with further oxidation reaction and

chemisorption of either WO_2 or WO_3 species. Therefore, the nucleation density was considered to be proportional to the supersaturation of the WO_2 species.

$$Nucleation\ Density\ \alpha\ \ RT\left[\ln\left(\frac{p_{WO2,filament}}{p_{WO2,substrate}}\right)\right] \qquad [3]$$

Based on this proposed theory, the equilibrium calculations were performed by calculating the equilibrium gas phase concentrations of WO_2 and WO_3 gas phase species at filament and substrate equilibrium conditions. Due to the lack of interfacial energy data of tungsten oxide, qualitative dependence of nucleation density on the partial pressure of oxygen, filament temperature and substrate temperature were obtained from the calculated equilibrium mole fractions of WO_2 and WO_3. As shown in figure 6a, there is an increase in the gas phase supersaturation of WO_2 and WO_3 species with increase in the partial pressure of oxygen with both filament temperature and substrate temperature remaining constant (1950 K and 823 K respectively). Different experiments were performed by changing the partial pressures of oxygen at constant substrate and filament temperatures and the nanowire densities were computed from the SEM images of the as-grown nanowires on the substrates. As shown in Figure 6b, there is a gradual increase in the nanowire density of nanowires with increase in the partial pressure of oxygen in agreement with the theoretically obtained qualitative trend. All the experiments were performed at lower partial pressures of oxygen (0.016 torr to 0.18 Torr) and nanowires with diameter in the range of 40 to 60 nm and lengths of about 5 microns were synthesized in all the cases. At higher partial pressures of oxygen (greater than 1 Torr), nanowires of different morphologies are synthesized.

More experiments are needed to understand the effect on nanowires morphology and density at higher partial pressures of oxygen. Theoretical calculations also showed that there is great influence of substrate temperature on the nucleation density. As shown in Figure 7a, there is a decrease in gas phase supersaturation of WO_2 and WO_3 species with increase in the substrate temperature. Experiments were performed in the temperatures ranging from 823 K to 1173 K keeping the filament temperature and pressure constant. As shown in figure 7b, there is decrease in the nanowire density with increase in the substrate temperature. At lower substrate temperatures, high supersaturation of gas phase species resulted in tungsten oxide nanowire arrays which were observed experimentally. At higher substrate temperatures, lower supersaturation of gas phase species resulted in low density nanowire mats. These experimental results clearly suggest that the qualitative trends of supersaturation of gas phase species obtained from the proposed model are consistent with the experimentally obtained nanowire densities indicating the validity of the proposed model. As shown in Figure 6a and 7a, theoretical model shows that the supersaturation of WO_2 species is higher compared to WO_3 species. This was also observed from the XRD data of the nanowires which showed that the nanowires are deficient in oxygen, and oxidation of the nanowires synthesized substrate in an oven changed the color and the phase to WO_3.
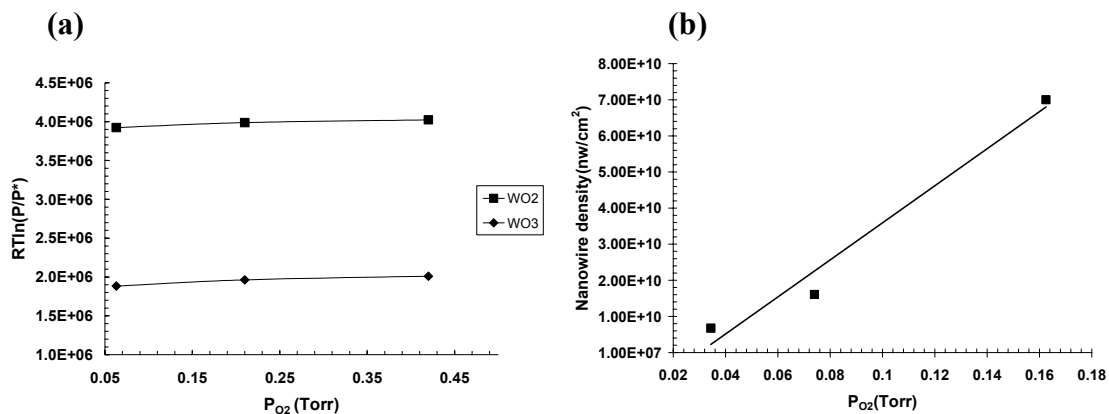
(a) **(b)**

Figure 6. Effect of nanowire density as a function of partial pressure of oxygen. (a) Theoretically estimated supersaturation of tungsten oxide (WO_3 and WO_2) species as a function of partial pressure of oxygen. (b) Experimentally determined effect of partial pressure of oxygen on nanowire density at lower substrate temperatures (823 K) and filament temperature (1950 K)
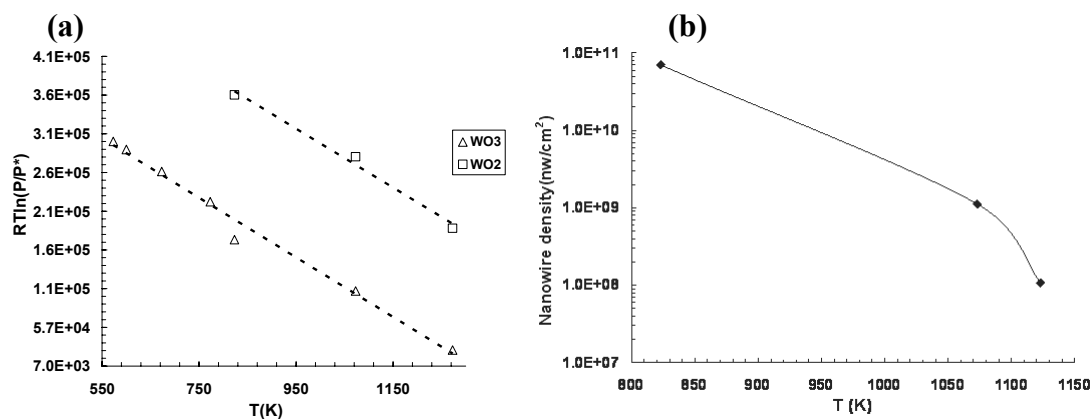
(a) **(b)**

Figure 7. Effect of nanowire density as a function of substrate temperature. (a) Theoretically estimated supersaturation of tungsten oxide (WO_3 and WO_2) species as a function of substrate temperature. (b) Experimentally determined effect of nanowire density on the substrate temperature

Dispersion Behavior Studies

The sedimentation studies were performed by observing the dispersions over several hours. Optical images taken at different times showed that tungsten oxide nanoparticles agglomerate and sediment out of the solution within few hours. Tungsten oxide nanowires remain in the solution for longer periods of time and no sediment or any kind of agglomeration is noticed for longer periods of time. Representative optical images of the nanowires and nanoparticle bottles are not shown here. Scanning Electron Microscopy (SEM) was used to understand the agglomeration patterns of nanowires and nanoparticles in the dispersion. As shown in Figure 8a, the 30 nm size nanoparticles agglomerated into micron size spherical agglomerates. In the case of nanowire

dispersions, the SEM images in Figure 8b show the presence of only individual nanowires with diameters in the range of 40 to 60 nm and lengths of about 5 μm. It clearly suggests that there is no agglomeration of nanowires in the solution. Similar kind of behavior was observed It can be confirmed that the thicker nanowires and some agglomerates seen in the sediment of the nanowire dispersion were formed during the synthesis of the material in the reactor and not in the solution. More in-depth in-situ characterization of agglomeration patterns of the nanowire dispersions using light scattering techniques are presently being performed and will be reported elsewhere.
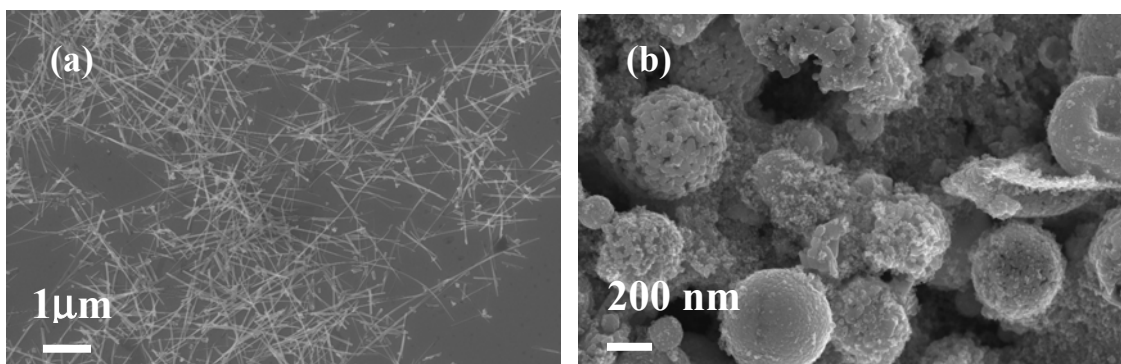

Figure 8. SEM images of nanowires and nanoparticles agglomeration patterns in Dimethyl Formamide (DMF) (a) Well dispersed nanowires in the DMF without any big agglomerates and thicker nanowires. (b) Dispersed tungsten oxide nanoparticles in the DMF solution showing big balls of agglomerates of individual nanoparticles

Conclusions

In summary, we successfully demonstrated the large scale synthesis of nanowires with different morphologies (nanowire mats, nanowire arrays and ball shaped structures with nanowires) on both amorphous quartz substrate and FTO substrates. Also, the as-synthesized nanowires were confirmed to be oxygen deficient $W_{18}O_{49}$ phase and subsequent oxidation of these substrates in an oven changed the phase to WO_3 which was indicated by a change in color from blue to green. We are the first to demonstrate a thermodynamic model for the nucleation density of these tungsten oxide nanowires which was consistent with the experimentally obtained nanowire densities at different process conditions. The proposed model predicted the large dependence of nucleation density on both the substrate temperature and partial pressures of oxygen which was consistent with the experimental findings. Also, we demonstrated that nanowires disperse better and show no signs of agglomeration and sedimentation compared to nanoparticles in organic solvents.

References

1. C. C. Lia, F. R. Chen, R. F, J. J. Kai, *Solar Energy Materials & Solar Cells,* 90, 1147 (2006)
2. C. J. Jin, T. Yamazaki, Y. Shirai, T. Yoshizawa, T. Kikuta, N. Nakatani, H. Takeda, *Thin Solid Films,* 474, 255 (2005)
3. E. L. Miller, B. Marsen, B. Cole. M. Lum, *Electrochem. Solid-State Lett.*, 9 (7), G248 (2006)
4. K. Liu, D. T. Foord, L. Scipioni, *Nanotechnology* 16, 10 (2005)
5. S. Vaddiraju, H. Chandrasekaran, M. K. Sunkara, *J. Am. Chem. Soc.*, 125 (36), 10792 (2003)
6. H. Qi, C. Wang, J. Liu, *Adv. Mater.*, 15, 411 (2003)
7. Y. Jin, Y. Zhu, R. L. D. Whitby, N. Yao, R. Ma, P. C. P. Watts, H. W. kroto, D. R. M. Walton, *J. Phys. Chem. B*, 108, 15572 (2004)
8. S. J. Wang, C. H. Chen, R. M. Ko, Y. C. Kuo, C. H. Wong, C. H. Wu, K. M. Uang, T. M. Chen, B. W. Liou, *Appl. Phys. Lett.*, 86, 263103 (2005)
9. K. Hong. W.Yiu, H. Wu, J. Gao, M. Xie, *Nanotechnology*, 16, 1608 (2005)
10. Z. Liu, Y. Bando, C. Tang, *Chem. Phys. Lett.*, 372, 179 (2003)
11. Z. Xiao, L. Zhang, X.Tian, X. Fang, *Nanotechnology*, 2005, 16, 2647-2650
12. J. Liu, Y. Zhao, Z. Zhang, *J. Phys. Condens. Mater*, 15, L453 (2003)
13. G. Gu, B. Zheng, W. Q. Han, S. Roth, J. Liu, *Nano Lett.*, 2 (8), 849 (2002)
14. Y. Q. Zhu, W. Hu, W. K. Hsu, M. Terrones, N. Grobert, J. P. Hare, H. W. Kroto, D. R. M. Walton, H. Terrones, *Chem. Phys. Lett.*, 309, 327 (1999)
15. Y. Li, Y. Bando, D. Golberg, *Adv. Mater.,* 15, 1294 (2003)